HHS Public Access

Author manuscript

J Nutr Biochem. Author manuscript; available in PMC 2022 December 01.

Published in final edited form as:

J Nutr Biochem. 2021 December ; 98: 108832. doi:10.1016/j.jnutbio.2021.108832.

Ceramide Synthase 6 mediates sex-specific metabolic response to dietary folic acid in mice

Keri Barron[1], **Besim Ogretmen**[2], **Natalia Krupenko**[1,3,*]

[1]Nutrition Research Institute, University of North Carolina at Chapel Hill, Kannapolis, NC 28081, USA

[2]Department of Biochemistry & Molecular Biology, Hollings Cancer center, Medical University of South Carolina, 173 Ashley Avenue, Charleston, SC 29425, USA

[3]Department of Nutrition, University of North Carolina at Chapel Hill, Chapel Hill, NC 27599, USA

Abstract

Objective—Folic acid-fortified foods and multi-vitamin supplements containing folic acid (FA) are widely used around the world, but the exact mechanisms/metabolic effects of FA are not precisely identified. We have demonstrated that Ceramide Synthase 6 (CerS6) and $C_{16:0}$-ceramide mediate response to folate stress in cultured cells. Here we investigated the dietary FA effects on mouse liver metabolome, with a specific focus on sphingolipids, CerS6 and $C_{16:0}$-ceramide.

Methods—Wild-type and CerS6$^{-/-}$ mice were fed FA-deficient, control, or FA over-supplemented diets for 4 weeks. After dietary treatment, liver concentrations of ceramides, sphingomyelins and hexosylceramides were measured by LC-MS/MS and complemented by untargeted metabolomic characterization of mouse livers.

Results—Our study shows that alterations in dietary FA elicit multiple sphingolipid responses mediated by CerS6 in mouse livers. Folic acid-deficient diet elevated $C_{14:0}$-, $C_{18:0}$- and $C_{20:0}$- but not $C_{16:0}$-ceramide in WT male and female mice. Additionally, FA over-supplementation increased multiple sphingomyelin species, including total sphingomyelins, in both sexes. Of note, concentrations of $C_{14:0}$- and $C_{16:0}$-ceramides and hexosylceramides were significantly higher in female livers than in male. The latter were increased by FD diet, with no difference between sexes in total pools of these sphingolipid classes. Untargeted liver metabolomic analysis concurred with the targeted measurements and showed broad effects of dietary FA and CerS6 status on multiple lipid classes including sex-specific effects on phosphatidylethanolamines and diacylglycerols.

*Corresponding author. 500 Laureate Way, Kannapolis, NC 28081, USA. Fax: +1 704 250 5001. natalia_krupenko@unc.edu.

AUTHOR CONTRIBUTIONS

The experimental design, implementation and data analysis were conducted by K.B. and N.K. CerS6 KO mice were generated by B.O. The manuscript was written by K.B. and N.K. The results discussion and manuscript review were performed by K.B., N.K. and B.O.

CONFLICT OF INTEREST

None declared.

Conclusions—Our study demonstrates that both dietary FA and CerS6 status exhibit pleiotropic and sex-dependent effects on liver metabolism, including hepatic sphingolipids, diacylglycerols, long chain fatty acids, and phospholipids.

Keywords

Dietary folate; Sphingolipid; Ceramide synthase 6; Metabolome; Sex difference; Metabolic health

1. Introduction

Folic acid is a synthetic oxidized pro-vitamin form of the vitamin B_9, natural reduced dietary forms of which are collectively called folate [1]. Neither folic acid nor folate can be synthesized by higher animal's cells but the latter is absolutely required for cell function. Thus, vertebrate animals depend on dietary supply of folate to support metabolic needs. In animal cells, folate is present in its fully reduced tetrahydrofolate (THF) form and functions as a carrier of one-carbon groups. Folate-bound one carbon groups could be at different oxidation levels and are linked to N_5, N_{10}, or both nitrogen atoms of THF [2]. These folate derivatives function as precursors of, or as co-factors donating one-carbon groups in numerous biosynthetic reactions, including nucleotide biosynthesis, amino acid metabolism and methylation reactions [2–4]. The source of one-carbon groups loaded on tetrahydrofolate are amino acids, mostly serine, glycine and histidine [1]. Liver is the first organ encountered by absorbed folate and amino acids, and it is considered to be the main organ of folate metabolism [5, 6]. Inadequate intake of folate in humans contributes to folate deficiency which has widespread effects due to vitamin's role in fundamental cellular processes [7–9]. For this reason, multiple countries including US and Canada have introduced fortification of grain foods with synthetic pro-vitamin, folic acid (FA) with the goal to reduce incidence of neural tube defects [2]. Importantly, in the last two decades a concern has been raised that folate over-supplementation, especially in the form of FA, can be harmful, but studies so far delivered conflicting results [6, 10–12]. The NIH expert workshop (August 2019) which performed rigorous systematic review of available evidence of the FA/folate effects, concluded that comprehensive and stringent investigations are warranted to determine safety of excess FA intake and elevated folate status [13].

Recently, research from our lab has demonstrated that metabolic stress induced by the disruption of folate metabolism via folate withdrawal, impairment of folate enzymes, or by antifolate drugs (generally termed "folate stress"), results in upregulation of Ceramide Synthase 6 (CerS6) and elevation of $C_{16:0}$-ceramide in cultured cells (A549, HCT116, HepG2, etc.) [14, 15], indicating a metabolic connection between folate and sphingolipid pathways.

Sphingolipids, the second largest class of lipids in biological membranes, share a common structural element (the sphingoid base), comprise 10-20% of membrane lipids [16] and define the unique biophysical properties of these membranes [17, 18]. Sphingolipids are also involved in the regulation of fundamental cellular processes such as proliferation, differentiation, migration, survival and senescence, as well as response to stress [16, 19, 20]. Therefore, it is not surprising that sphingolipids have been implicated in the

development and progression of diseases including cancer, type 2 diabetes, cardiovascular and Alzheimer's disease [21–26]. Ceramides, sphingosine and sphingosine-1-phosphate are often investigated as regulatory or signaling lipids [22, 27], however recently such roles have also been proposed for complex sphingolipids [16].

Often viewed as central players in sphingolipid metabolism, ceramides are synthetized in cells *de novo*, starting from the condensation of serine and palmitoyl-CoA followed by reduction to dihydrosphingosine, N-acylation to dihydroceramide by ceramide synthases (CerSes), and final conversion to ceramide by dihydroceramide desaturase [24]. Ceramides can also be produced via degradation of pre-formed complex sphingolipids in the endolysosomal pathway by acid sphingomyelinase and glycosidases, and by ceramide synthases utilizing free sphingosine generated through the degradation of pre-formed complex sphingolipids and S-1P (salvage pathway) [24]. Six members of the ceramide synthase family (CerS1-6) have been identified [28, 29], and their functions and tissue distribution have been reviewed extensively [24, 28–30]. These enzymes carry out the same chemical reaction but differ in their preference for the specific acyl-CoA used, which results in the unique balance of different ceramides in cells and tissues. Multiple studies have shown that cellular effects of sphingolipids, in particular ceramides, depend on their specific structural characteristics, including acyl chain length [30, 31] and underscored ceramides roles in cardiovascular disease [26], metabolic syndrome [23] as well as alcoholic and non-alcoholic liver disease [32–35]. These investigations placed focus on ceramide synthases as attractive targets both in biomedical research and in development of novel therapeutic approaches for treatment of diseases [30, 36, 37].

CerS6, implicated in response to folate stress[14, 15], similar to another family member CerS5, preferentially produces C_{14}- and C_{16}-ceramides [29]. It is expressed in many tissues, but generally at low levels, and can be upregulated by various types of stress resulting in the increased production of $C_{16:0}$-ceramide and anti-proliferative/apoptotic response [38–41]. However, there is no information on whether the link between dietary folate, CerS6 and sphingolipid pathways functions in the whole organism. We hypothesized that, similar to cells in culture, the crosstalk between folate and sphingolipid pathways also operates in the whole animal and consequently FA deficient diet will result in an increase of $C_{16:0}$-ceramide in response to folate deficient diet.

We examined the effects of dietary folic acid supplementation (low, standard and high levels of FA) on the sphingolipid profiles and liver metabolome in WT and CerS6$^{-/-}$ mice to determine the broad effects of folate deficiency and over-supplementation on liver sphingolipids, as well as overall metabolism and to evaluate the role of CerS6 and ceramide in maintaining tissue homeostasis. Since liver is the primary site of folate metabolism and the main organ processing dietary folate, and it expresses CerS6 among other CerS, we initially limited our focus specifically on the changes to sphingolipid profiles and metabolome of the liver tissue.

2. Materials and Methods

2.1 Animals and husbandry

All animal experiments were approved by the Institutional Animal Care and Use Committee (IACUC) at the North Carolina Research Campus (NCRC). CerS6$^{-/-}$ mice were generated in Dr. Ogretmen's lab and we bred them back 5-6 generations to the C57B1/6NHsd mice purchased from Envigo (Indianapolis, IN). For dietary experiments animals were generated by breeding heterozygous (CerS6$^{+/-}$) males and females and offspring genotype was determined by PCR of lysed tails with specific primers (Supplementary Table 1). Wild type (CerS6$^{+/+}$) and knockout (KO, CerS6$^{-/-}$) littermates, both male and female, were randomized to dietary groups. Mice were group housed in microisolator cages under standard conditions (12h light/dark cycle, temperature- and humidity-control) with *ad lib* access to water and one of the three purified synthetic diets containing 14.4% kcal from fat, 66.5% kcal from carbohydrates, and 19.1% kcal from protein, and differing only in the amount of folic acid (FA). All diets were purchased from Envigo: 1) folic acid deficient diet (FD, catalog number TD.95247) with no added FA and containing only residual 0.2 ppm FA coming from added protein; 2) control diet (Ctrl) with 2 ppm FA added (TD.160824), which is the level of FA supplementation in standard rodent chow, and 3) folic acid over-supplemented diet (FS) containing 12 ppm added FA (TD.160825). The amino acid sources (casein and L-cystine) were consistent across diets, as were sources of carbohydrates (corn starch, sucrose, maltodextrin), fat (soybean oil) and all vitamins except FA. Wild type (WT) and CerS6$^{-/-}$ (KO) littermates, both male and female, were placed on respective diets at 10 weeks of age and maintained on the diets for 4 weeks. Our previous studies have shown that after two weeks on the FD diet, total blood folates in mice were reduced 2.2-fold, liver folates were lower by 18% and lung folates dropped by 2.7 fold [42]. Thus, the dietary exposure was chosen to be 4 weeks in order to detect early responses to alterations of dietary FA in the liver.

Body mass and composition (lean and fat mass) were assessed before and after dietary exposure using the EchoMRI-130 Body Composition Analyzer. At the end of dietary exposure (14 weeks of age), mice were fasted for 4 hours before being euthanized, and blood was drawn via retro-orbital bleed. Blood and major tissues were collected, sections of liver were fixed in buffered formalin and the remaining tissues were snap-frozen in liquid nitrogen for further analysis.

2.2 Western blot assays

Western blot assays were used for analysis of CerS6 expression and genotype confirmation (Supplementary Figure 1). Fragments of frozen livers (~30 mg) were homogenized using Dounce homogenizer in 750 μl of RIPA buffer containing phosphatase and protease inhibitor cocktail (1:100, Sigma-Aldrich, St. Louis, MO), sonicated and centrifuged (20,000 x g, 5 min, 4°C). The supernatant was stored at −80°C. Aliquots of 20 μg of total protein were subjected to SDS-PAGE followed by immunoblot with corresponding antibodies. All antibodies were diluted in 3% BSA blocking buffer. Membranes were washed 4 times with 2% TWEEN-20 in TBS. Blots were developed with SuperSignal West Pico

Chemiluminescent substrate and analyzed using the Odyssey Fc infrared scanner from LI-COR.

2.3 LC-MS/MS analysis of sphingolipids

Aliquots of frozen tissues were homogenized in PBS using Dounce homogenizer. Homogenate volumes containing 1 mg of total protein were immediately frozen and stored at −80 ° C. Sphingolipid concentrations were measured using UHPLC-MS/MS or SFC-MS/MS methodology as previously described [43], by the MUSC Lipidomics Shared Resource. Measurements are presented as mean ± SEM, pmol/mg of tissue protein. Measurements of hexosylceramides include glucosyl- and galactosyl-ceramides, but not lactosylceramide species.

2.4 Plasma Markers

Blood (after 4 hours fasting) was collected into EDTA-containing tubes and plasma was separated via centrifugation at 6,000 x g for 10 minutes at 4°C. Plasma triacylglycerol, cholesterol and glucose were measured using Thermo Fisher Scientific Infinity colorimetric assays with appropriate standards (Stanbio glucose standard (100mg/dl), Pointe Scientific TG standard (200mg/dl), and Pointe Scientific Cholesterol standard (200mg/dl)). All samples were run in triplicate with n=5 per group. Plates were read using the BioTek Synergy HT plate reader and validated with internal controls of pooled plasma.

2.5 Histology

Liver sections fixed in 10% formalin were embedded in paraffin blocks and 5 μm sections from the blocks were placed on slides, deparaffinized, re-hydrated and stained with hematoxylin and eosin according to standard protocol. Images were taken on Keyence BZ-X710 All-in-one fluorescence microscope at 2X, 10X, and 20X magnification.

2.6 Untargeted Metabolomics Analysis

Untargeted metabolomic analysis was performed by the commercial service provider Metabolon® (Durham, NC). Snap-frozen tissue samples were subjected to extraction with methanol and divided into aliquots for further analysis by ultrahigh performance liquid chromatography/mass spectrometry (UHPLC/MS). The global biochemical profiling consisted of four unique arms covering identification of both hydrophilic and hydrophobic compounds under both positive and negative ionization conditions as described [44, 45]. Chromatographic conditions for polar compounds detection in the positive ionization mode included Waters BEH C18 1.7μm, 2.1 x 100 mm column, 0.1% formic acid and 0.05% PFPA in water, pH ~2.5 as Mobile Phase A and 0.1% formic acid and 0.05% PFPA in methanol, pH ~2.5 as Mobile Phase B. Linear gradient from 5% to 80% B over 3.35 minutes was used for metabolites elution. For lipid compounds identification in the positive ionization mode, the same column type was used with 0.1% formic acid and 0.05% PFPA in water, pH ~2.5 as Mobile Phase A and 0.1% formic acid and 0.05% PFPA in 50% methanol/50% acetonitrile, pH ~2.5 as Mobile Phase B, with elution gradient from 40% to 99.5% B over 1.0 minute, then hold 99.5% B for 2.4 minutes. For detection in negative ionization mode, separation was also performed on the Waters BEH C18 1.7μm, 2.1 x

100 mm column, with 6.5 mM ammonium bicarbonate in water, pH 8 as Mobile Phase A and 6.5 mM ammonium bicarbonate in 95% methanol/5% water as Mobile Phase B using a linear gradient from 0.5% to 70% B over 4 minutes, then to 99% B in 0.5 minutes. Negative ionization detection of polar compounds was carried using separation on Waters BEH Amide 1.7um, 2.1 x 150mm column with Mobile Phase A as 10 mM ammonium formate in 15%water/5% methanol/80% acetonitrile (effective pH 10.16 with NH4OH) and Mobile Phase B as 10 mM ammonium formate in 50% water/50% acetonitrile (effective pH 10.60 with NH4OH). Elution was carried out via a linear gradient from 5% to 50% B in 3.5 minutes, then linear gradient from 50% to 95% B in 2 minutes. Metabolites were identified by automated comparison of the ion features in the samples to a reference library of chemical standards characteristics which included retention time, m/z (mass/charge) ratio, predominant adducts and in-source fragmentation and associated spectra. Measurements on 736 identified metabolites, including two folate derivatives (FA, and 7,8-dihydrofolate) were provided for this sample set.

2.7 Statistical analysis

For statistical analysis of differences between two groups Student's t-test was performed using GraphPad software. For the statistical analysis of differences between three or more groups, one-way ANOVA was used with Sidak's multiple comparisons test to determine differences between specific groups. Statistical analysis of the fixed effects of sex, genotype or diet, as well as their pair-wise interactions and the interaction of all three factors were completed by Metabolon® using ANOVA comparisons (complete data are included in the Supplementary Table 2). Metabolomics data were also analyzed using Qlucore Omics Explorer v.3.4 software (Qlucore, Lund, Sweden).

3. Results

3.1. Alterations of dietary folic acid result in significant changes of liver folates

As expected, untargeted metabolomics analysis revealed that higher FA in the animals' diets resulted in the increased FA concentrations in both male and female livers (Figure 1a). The tissue concentrations of 7,8-Dihydrofolate (DHF) significantly increased with elevation of dietary FA in WT and KO males and in KO females, but changes in WT females did not reach statistical significance (Figure 1b). The liver concentrations of FA and 7,8-DHF were lower on FD vs CTRL diet by 69% and 57%, correspondingly, in WT females and by 79% -81% in KO females (Figure 1c). In males, differences of tissue FA and DHF on FD compared to CTRL diet were even stronger, decreased by 88 and 86%, correspondingly, in WT and 86 and 87% in KO mice, confirming the lowest liver folate pools on FD diet in our experiments. Folic acid over-supplemented diet increased liver FA and DHF pools in both sexes by 16% to 91%, compared to CTRL diet. This resulted in 3.8- and 3.2-fold increases of FA and 7,8-dihydrofolate respectively, in WT females between FD and FS diets, and 7.3- and 6.8-fold elevations in KO females between FD and FS diets (Figure 1c). As in the case of FD diet, responses to FS diet in males were stronger than in females, and concentrations of FA and 7,8-DHF in WT livers were 12- and 7.4-fold higher, respectively, while in the KO livers 10.7- and 14.2-fold differences were observed (Figure 1c).

Surprisingly, 5-methyl-tetrahydrofolate, 5M-THF, one of the major reduced folates and the folate storage form in liver, did not show significant differences between FD and CTRL diets (Figure 1d). Furthermore, liver concentrations of 5M-THF were reduced by FS diet compared to CTRL diet in males by 53% and 45% in WT and KO, respectively, and in females by 46% and 51% in WT and KO respectively (Figures 1c & 1d). Importantly, in one of the peripheral tissues, testes, 5M-THF was increased dose-dependently from FD to CTRL to FS diet both in WT and KO males (Figure 1d).

Concentrations of formiminoglutamate (FIGLU, a product of histidine catabolism, requiring tetrahydrofolate for its degradation, and used in the past as a marker of folate deficiency[46]) were elevated in the folate-deficient livers and reduced in folate over-supplemented tissues, consistent with the role of tetrahydrofolate as the acceptor of the formimino group from FIGLU (Supplementary table 1).

3.2 CerS6 knockout reduced accumulation of fat mass in male mice, independent of FA supplementation

Animals body mass and composition were evaluated both before and after dietary treatment. There were no significant differences in the pre-diet body weight between any of the treatment groups, except the KO-FS male group. Due to random assignment of littermates to dietary treatment groups, the average pre-diet weight of males in the KO-FS group was slightly lower than in the KO-Ctrl group and this difference remained after the dietary treatment (Figure 2), resulting in the absence of significant difference in the change of body weight between the groups (Figure 2). At the end of dietary treatment WT male mice gained more weight and showed higher percent of fat mass than their KO counterparts on all diets. Additionally, WT-FS males gained more weight and had significantly higher fat mass than WT-Ctrl group. Simple regression analyses of the pre-diet body weight among the three male KO groups and several of the post-diet tested parameters, including change in body weight, change in percent fat mass, liver FA concentration, or dihydrofolate concentration, have shown absence of co-variation (Supplementary Figure 2). Thus, pre-diet body weight was not considered as a co-variate in subsequent analyses.

Compared to male mice, WT females gained less weight and were overall leaner than males on all diets, however KO females had overall higher percent of fat mass than KO males, independent of diet. Additionally, there were no differences between WT and KO females in the gain of body mass, or in percent of fat mass (Figure 2), indicating that CerS6 knockout does not affect weight gain and fat mass increase in females on these diets.

Measurements of plasma glucose and cholesterol as well as evaluation of liver/body weight ratios did not show significant differences between genotypes or dietary treatments for both sexes (Supplementary Figure 3). Histological examination of livers from WT and KO animals on different diets did not show obvious differences between genotypes or any dietary treatments (Supplementary Figures 4 & 5).

3.3 Alteration of dietary folic acid significantly affected liver sphingolipids

3.3.1 Both CerS6 knockout and folate deficiency affect ceramide profiles of liver—

As expected, $C_{14:0}$- and $C_{16:0}$-ceramides were significantly lower (2-3-fold) in livers of CerS6 KO compared to WT mice for both sexes (Figure 3a). Consumption of FD diet significantly increased $C_{14:0}$-ceramide only in male WT mice. Concentrations of $C_{16:0}$-ceramide in FD livers did not differ significantly from CTRL diet livers in both sexes (Figure 3a), although male WT mice fed FS diet had a significant decrease in $C_{16:0}$-ceramide compared to those fed the Ctrl diet. Of note, both $C_{14:0}$- and $C_{16:0}$-ceramides were significantly higher in WT females than in WT males. In KO mice $C_{14:0}$-ceramide was also significantly higher in FD females than in males (differences on CTRL and FS diets did not quite reach the significance), but there was no difference in $C_{16:0}$-ceramide between sexes (Figure 3b).

$C_{18:0}$-, $C_{18:1}$-, $C_{20:0}$-, and $C_{20:1}$-ceramides were progressively decreased with increase of FA supplementation, while C_{22}- and $C_{22:1}$-ceramides were significantly increased on FS compared to CTRL diet in both sexes. Despite the similar pattern of response to FA, liver concentrations of 18-carbon chain ceramides were significantly higher in females, while both 20- and 22-carbon chain ceramides were significantly higher in males. Additionally, very-long-chain ceramides ($C_{24:0}$-, $C_{26:0}$- and $C_{26:1}$) were increased in male KO livers compared to WT on CTRL diet, but not on FD diet (Supplementary Figure 7a). No such elevation was observed in females (Supplementary Figure 7b). Overall, the total ceramide concentrations were not significantly different between different genotypes and different diets, both in males and females with the exception of female KO FD mice compared to female KO FS mice (Supplementary Figure 7).

3.3.2 Hexosylceramides are modulated by dietary folic acid—

Similar to $C_{14:0}$- and $C_{16:0}$-ceramide, hexosylceramides with $C_{14:0}$- and $C_{16:0}$-acyl chains were significantly higher in WT female livers than in male (Figure 4a). Total HexCer levels were more similar between male and female mice with only one group, KO-FD, demonstrating a significant difference between male and female mice (Figure 4a). Interestingly, concentrations of $C_{16:0}$-hexosylceramide in WT females were 2.4 times higher than in WT males, with both FD and FS diets further increasing this difference to 2.6-fold. $C_{14:0}$-hexosylceramide showed even greater differences between sexes and also increased in response to FD diet in both WT and KO mice (Figure 4a). The FD diet significantly increased $C_{20:0}$- and $C_{22:0}$-hexosylceramides in male WT mice compared to Ctrl or FS diet fed mice, however in female mice this effect was seen in KO animals but did not reach significance in the WT (Figure 4b). There were few significant changes in other hexosyl ceramides in CerS6 KO male livers, with exception of $C_{24:1}$-HexCer which was significantly lower on FS diet. Similarly, total HexCer concentrations were lower in KO vs WT males on every diet (the differences, however, did not reach statistical significance, Supplementary Figure 8). On the other hand, in females several HexCer species ($C_{16:0}$, $C_{18:1}$, $C_{20:1}$, $C_{22:1}$, $C_{24:0}$) demonstrated significantly higher concentrations on the FD than on FS diet for both genotypes (Supplementary Figure 8). Total HexCer concentrations were significantly increased due the FD diet in WT and CerS6 KO mice of both sexes. Furthermore, in females the total HexCer concentrations were significantly lower in KO-Ctrl compared to WT-Ctrl mice (Supplementary Figure 8).

3.3.3 Excess of dietary folic acid significantly increased sphingomyelin concentrations while CerS6 KO has little effect on sphingomyelins—

FS diet elevated multiple sphingomyelin species in WT and KO mice: $C_{20:0}$, $C_{20:1}$, $C_{22:0}$, $C_{22:1}$ and $C_{24:1}$ in both sexes (Figure 5), as well as $C_{18:1}$ in males and $C_{24:0}$ and $C_{26:1}$ in females (Supplementary Figure 9). Total sphingomyelin concentrations were higher in females, compared to males and also were significantly elevated in both sexes by folic acid over-supplementation (Figure 5). However, no significant differences in $C_{14:0}$- and $C_{16:0}$-sphingomyelins at different dietary FA levels were found in either WT or KO males (Supplementary Figure 9). Wild-type females demonstrated significantly elevated $C_{14:0}$- and $C_{16:0}$-sphingomyelins on FS compared to FD diet only (Supplementary Figure 9), and similar increase of $C_{18:0}$- and $C_{18:1}$-SM was found in males but not in females (Supplementary Figure 9).

3.3.4 Sphingosine and sphingosine-1-phosphate are not affected by either dietary folic acid or genotype.—

Sphingosine (Sph) was significantly elevated by consumption of FD diet in both male and female KO mice (Supplementary Figure 10). There were no changes in WT mice. No significant differences in sphingosine-1-phosphate (Sph-1-P) concentrations were observed in WT or KO animals on different diets.

3.4 Both CerS6 knockout and dietary FA induce sex-dependent alterations of liver metabolome.

3.4.1 Mouse liver metabotypes show significant differences based on sex, genotype and diet, with diet effects being less pronounced—

Untargeted metabolomic analysis provided measurements of 736 named biochemicals in mouse liver tissues. Statistical comparisons of the measured metabolites using principal component analysis (PCA) and hierarchical clustering (HC) demonstrated the strongest separation of the metabotypes by sex (Figure 6a) and genotype (Figure 6b), with separation by diet being also discernible (Figure 6c). To that end, 550 metabolites were statistically significantly ($p \leq 0.05$) different between male and female mice regardless of diet and genotype whereas 298 and 273 metabolites differed significantly between dietary interventions and genotype, respectively (Supplementary Figure 11a). Heat map analysis also demonstrates clear separation of metabotypes by sex, genotype and by diet (Figure 6d).

Random forest analysis, an unbiased supervised classification approach which splits the samples into groups based on the biochemicals providing the best separation between groups, showed a predictive accuracy of 64% compared to 8.3% due to random chance alone, when all 12 groups were included in the analysis (Supplementary Figure 11b). The biochemical importance plot lists the top 30 metabolites which make the highest contribution to the separation of group's metabotypes (Supplementary Figure 12). Thus, the concentrations of ceramides and sphingomyelins with C_{16}-acyl chain (reflect the genotype of the groups), folate derivatives and formiminoglutamate (reflect the dietary supplementation and animal's folate status), as well as several glycerophosphoethanolamines (linked to phosphatidylcholines required for sphingomyelin biosynthesis) are the strongest discriminators between groups' metabotypes.

3.4.2 Not only ceramide and ceramide-based lipids, but also free fatty acids, diglycerides and phospatidylethanolamines are altered in CerS6 KO mice— Similar to our targeted measurements of ceramides, sphingomyelins and hexosylceramides, untargeted metabolomics demonstrated significant decreases in C_{16}-acyl chain containing sphingolipids in the CerS6 KO mouse livers (Supplementary Table 3). Decreases of 30 – 65 % were observed for most of these sphingolipids (d18:0/16:0; d18:1/16:0; d16:1/16:0; d18:1/16:0(2OH); d18:2/16:0), while N-palmitoyl-heptadecasphigosine (d17:1/16:0) decreased over 90% and glycosyl-N-palmitoyl-sphingosine dropped more than 75%, in both males and females (Supplementary Table 3a). C_{16}-sphingomyelins (d18:1/16:0; d16:1/16:0; d18:1/16:1 and C17:1/16:0) showed similar decreases (Supplementary Table 3b). Slight changes (<30%) in a few very-long-chain ceramides were noted ($C_{20:0}$, $C_{22:0}$ and $C_{24:1}$), but most of these did not reach significance. At the same time very-long-chain sphingomyelins ($C_{18:0}$, $C_{22:0}$, $C_{24:0}$) demonstrated statistically significant increases of up to 70% with elevation in females seen more often (Supplementary Table 3b). Overall, multiple sphingomyelin species in female livers, both WT and KO, were significantly higher than in male livers, reaching over six-fold differences, with very few showing similar or two-fold lower concentrations (Supplementary Table 3b).

Importantly, knockout of CerS6 induced changes in other lipid classes, besides sphingolipids. Elevation of phosphatidylethanolamines (16:0/16:0, 16:0/18:0, 16:0/18:1, 16:0/18:2, 16:0/20:4, 16:0/22:6, 18:0/18:1, 18:0/18:2,18:0/20:4, 18:0/22:6, 18:1/18:2, 18:1/20:4, 18:1/22:6,18:2/18:2 and 18:2/20:4) was found both in males and females, with more abundant changes in males (Table 1). On the contrary, diacylglycerols (with acyl chains $C_{16} – C_{22}$), as well as long chain ($C_{14} – C_{22}$) and polyunsaturated fatty acids (20:3n3 or n6; 22:5n6; 20:2n6; 22:2n6) were significantly reduced, also more frequently in males than females (Supplementary Tables 4 & 5). Interestingly, phosphatidylcholines showed significantly fewer alterations in both sexes, with only 16:0/18:2 and 16:0/18:3n6 being changed in opposite direction to corresponding diacylglycerols and only in males (Supplementary Table 6).

3.4.3 Effects of sex, genotype and diet on liver metabolome, as well as their interactions are apparent from metabolomic data—Three-way ANOVA was used to analyze the metabolomics data to determine fixed effects of sex, genotype and diet on metabolite levels as well as interactions between the three factors (Supplementary Table 2). Out of 550 metabolites showing significant differences in liver concentrations between the sexes, 487 showed statistically significant differences ($p<0.01$) with the fold-differences ranging from 1.5 to over 20. The top 46 metabolites showing such effect are involved in amino acid metabolism, mannose and amino-sugar metabolism as well as lipid metabolism (Supplementary Tables 7 and 8). The fixed effect of genotype was linked to differences in 273 metabolites, with 173 of these showing significant differences ($p<0.01$, Supplementary Table 9). The top 46 metabolites in this group are presented by sphingolipids, phosphatidylethanolamines, acylcholines, diacylglycerols, and phosphatidylcholine (Supplementary Table 9). Fixed effect of dietary FA was found to significantly affect 298 metabolites with 167 of these with a $p<0.01$. Folic acid affected folate/one-carbon and multiple vitamins metabolism, amino acid metabolism,

glycogen metabolism, TCA cycle, purine metabolism and multiple branches of lipid metabolism (sphingolipid metabolism, fatty acid metabolism, phospholipid metabolism, lysolipid metabolism as well as bile acids metabolism, Supplementary Table 10 shows top 46 metabolites). Importantly, sex, genotype and diet displayed significant interactions with each other. Thus, significant genotype:diet interactions were shown for 86 metabolites involved in amino acid, nucleotide, carbohydrate and lipid metabolism (Supplementary Table 11). Significant sex:diet interactions indicating that dietary FA levels affected metabolites differently in males compared to females, irrespective of genotype, were shown for 113 metabolites (Supplementary Table 12 shows top 46 of them). This interaction was highly statistically significant ($p \leq 0.01$) for metabolites of lipid pathways, such as polyunsaturated and monohydroxy fatty acids, lysophospholipids, ceramide, sphingomyelin and several phospholipids. Additionally, metabolites from glycolysis, pentose and glycogen pathways, glutathione, methionine and lysine metabolism, as well as several essential vitamin's intermediates displayed significant interactions. On the other hand, genotype:sex interactions were found for 143 metabolites. Among these, metabolites displaying highest statistical significance ($p \leq 0.01$) belong to the groups of ceramides and ceramide-derived sphingolipids, diacylglycerols, as well as some pentose metabolites, purine, pyrimidine and TCA cycle metabolites (Supplementary Table 13). Finally, 44 metabolites involved in amino acid, nucleotide, amino sugar and lipid metabolism were showing significant differences depending on all three factors: sex, genotype and diet (Supplementary Table 14).

4. Discussion

Folic acid is a synthetic pro-vitamin B_9 which is widely present in fortified foods and multivitamin supplements in numerous countries, however the precise effects of dietary FA on metabolism in humans (or animals in general) have not been evaluated. The August 2019 NIH expert workshop identified the pressing need to investigate the effects of FA supplementation and its mechanisms, establish dose-response relations, and causal nature of such relations[13]. Previously, we have demonstrated the crosstalk between folate and sphingolipid pathways which is mediated by CerS6 and C_{16}-ceramide, in cell culture models. Here we investigated the effects of dietary FA in a whole animal model using CerS6 KO and WT mice. Folate stress was induced in the animals by feeding them with purified Envigo diets that contained no FA added for folate-deficient diet (FD), or 12 ppm FA for folate over-supplemented diet (FS). Effects of these diets were compared to control diet with 2 ppm FA (average rodent chows contain 2-3 ppm FA). Since we are interested in the animal response to physiological folate restriction and not to severe vitamin deficiency, we abstained from the use of antibiotic in the FD diet.

Untargeted metabolomic analysis of the liver tissues has confirmed that, over the course of 4 weeks, selected diets were able to alter liver folate pools in all mice. We observed both sex- and genotype-dependent differences in response to alterations of dietary FA. Liver FA accumulation showed dose-dependency in both sexes and both genotypes. However, while the tissue FA concentrations on FD diet were slightly higher in females compared to males (without reaching significance), on FS diet male livers accumulated higher concentrations of FA than female livers of the same genotype, and for each sex, KO mice accumulated more FA in livers than their WT counterparts. Thus, fold-increases of liver FA in males

on FS vs FD diets were 12 and 10.7 for WT and KO mice respectively, while in females fold-increases were 3.8 and 7.25 for WT and KO respectively (Figure 1 a & d). Similarly, for 7,8-DHF fold-increases on FS vs FD diet were 7.4 and 14.2 in WT and KO males, respectively, and only 3.2 and 6.8 in WT and KO females, respectively (Figure 1 b & d).

Tissue levels of folate coenzymes are defined by the dietary supply of the vitamin, its transport, as well as by folate enzymes and binding proteins (the cell concentration of these is higher than the total folate concentration [47]). Two major facilitative transporters, the ubiquitously expressed reduced folate carrier (RFC) and the proton-coupled folate transporter (PCFT), which has more limited tissue expression profile, support the transport of folates and FA into the tissue cells [48]. While for RFC a rather complex transcriptional and post-transcriptional regulation of protein levels has been established [49], the PCFT is significantly less studied and for both transporters no information on sex differences in expression or regulation is currently available. Thus, the understanding of how exactly folate transport and metabolism are regulated in different sexes is still missing. Moreover, the fact that on FS diet CerS6 knockout animals accumulated more FA or DHF than WT mice of the same sex (Figures 1a & b) points to potential involvement of ceramides in transporters or DHFR activity regulation.

Liver concentrations of the major transport and storage form of folate, 5-MTHF, did not show significant differences between genotypes or sexes (Figure 1c). However, we observed a decrease in tissue 5-MTHF concentrations both in males (55% and 60% for WT and KO, respectively) and in females (64% and 50% for WT and KO, respectively) at the highest FA supplementation (Figures 1 c & d). While counter-intuitive at the first glance, our data agree with the published observations for WT and methylenetetrahydrofolate reductase-deficient mice ($MTHFR^{+/-}$) that were fed diets over-supplemented with FA (20 ppm FA) for 6 months [11]. This earlier study found that FA inhibits the activity of MTHFR (the only enzyme producing 5-MTHF) *in vitro*, reduces overall MTHFR concentrations in over-supplemented animals and increases phosphorylation of the enzyme reducing its activity [11]. These mechanisms diminished liver methylation capacity, mobilized methyl group use from choline and betaine, altered expression of one-carbon and lipid metabolism genes and led to hepatocyte degeneration. In this regard, our experiments demonstrate that same metabolic perturbations in liver methyl group metabolism are noticeable much earlier, within four weeks of FA over-supplementation, and argue for caution with regard to use of high-dose FA supplements even for a shorter time.

Interestingly, 5M-THF in a peripheral tissue, specifically in the testes, was increased dose-dependently with FA supplementation. This could be explained by the fact that all peripheral tissues are exposed to blood folate only, where 83 - 95% is represented by 5-MTHF [42, 50–52]. Thus, peripheral tissues may be less affected by the inhibitory effects of high dietary FA on MTHFR. Of note, testes were selected for metabolomic analyses because our early experiments indicated histological abnormalities in male reproductive organs of CerS6 KO mice. However, no differences in FA metabolites were found between WT and $CerS6^{-/-}$ testes.

In contrast to the MTHFR deficiency study, our work found no major histopathological changes related to specific diet or genotype in our animals, that could be explained by shorter duration of the dietary treatment (Supplementary Figures 4 & 5). Only occasional lipid droplets formation could be seen on any of the 3 diets, though more often in livers of FA-deficient mice. Importantly, livers of the KO FA-supplemented animals of both sexes were protected from steatosis. This observation is consistent with the previously demonstrated involvement of CerS6 in lipid droplet biology [53]. Indeed, while the above referenced study of FA over-supplementation has shown increase of liver and spleen mass, as well as liver steatosis in animals after six months on FA- over-supplemented compared to control diet [11], in our experiment liver mass did not differ between groups and no significant differences in plasma glucose and cholesterol concentrations were observed (Supplementary Figure 3).

Overall, our data show perturbations in liver folate metabolism of mice supplemented with high doses of FA, which could also be an important issue for people taking high doses of this vitamin form, especially for prolonged periods. However, this point requires more thorough and focused investigation as well as consideration of the effects of different vitamin forms and of the metabolic differences between the species (mice vs humans).

Despite the fact that at the end of dietary treatment the animals body weights were not different between different dietary groups, the KO males on all diets gained significantly less weight than WT males and had significantly lower fat mass (Figure 2). The protection of KO males from weight gain is in agreement with the results obtained in a different CerS6 KO model, where protection from obesity and improvement of glucose tolerance were found [54], thus, spurring the interest in pharmacological inhibition of CerS6 for development of therapeutic approaches to combat obesity and type 2 diabetes. Subsequent investigation of the CerS6 downregulation using CerS6 targeting antisense oligonucleotides confirmed lower weight gain and protection from insulin-resistance in the CerS6 knockdown group [55]. Experiments with myocyte targeted double-knockout of CerS5 and CerS6 did not show alterations in adiposity or systemic insulin sensitivity indicating that muscle C_{16}-ceramide plays minor role in overall control of adiposity or insulin resistance [56]. The mechanisms by which CerS6 and C_{16}-ceramide control weight gain and insulin resistance are not known. The simultaneous activation of anabolic and catabolic pathways of lipid metabolism found in epididymal white adipose tissue of CerS5 KO mice (also depletes C_{16}-ceramide) was hypothesized to result in futile metabolic cycle and improvement of adipose tissue balance [57]. Alternatively, C_{16}-ceramide produced specifically by CerS6 but not by CerS5, was shown to bind to the mitochondrial fission factor (Mff) at the outer mitochondrial membrane and promote mitochondrial fission which impairs mitochondrial function and induces insulin resistance [58]. In our case, the absence of CerS6-produced ceramide could promote highly efficient mitochondrial function that may help in fatty acids utilization and reducing storage. Interestingly, protection from weight accumulation by CerS6 knockout was not observed in female mice in our experiments. It should be noted that, almost all published studies have used only male mice in their experiments, thus the concept of “protection by CerS6 inhibition” requires further investigation of the CerS6 function. Importantly, sex differences in the $C_{16:0}$-ceramide response to obesity-inducing diet have been demonstrated for mouse livers [55], but no information on female’s body weight was presented. Thus, extremely

scarce information on dietary effects in females further underscores the importance of taking into account sex differences in response to dietary interventions as well as pharmacological interventions targeting ceramides.

The data generated in this study confirmed our hypothesis that in the whole animal, ceramides (and other sphingolipids) respond to alterations of dietary folic acid. Thus, folate depletion in WT male livers caused significant increase in $C_{14:0}$-ceramide concentrations, however $C_{16:0}$-ceramide concentrations were not significantly different between control and FD livers in WT animals of both sexes (Figure 3). The observed lack of $C_{16:0}$-ceramide elevation could be explained by the tight control of this sphingolipid mediator due to its role in lipotoxicity [59]. Additionally, ceramides are important regulatory molecules and their concentrations must be tightly controlled [60, 61]. Homeostatic concentrations of ceramides could be maintained via their conversion to complex sphingolipids, such as sphingomyelins and/or hexosylceramides, that could function as a safety mechanism protecting from damaging effect of response to dietary alterations [62, 63]. Potentially, re-distribution of ceramide to other tissues (including the lipoprotein particles in blood) could help control liver ceramide levels, however, this aspect merits a separate study.

Since we did not observe significant changes in $C_{14:0}$- and $C_{16:0}$- SM in male livers (Supplementary Figure 9), SM biosynthesis is likely not the mechanism of ceramide concentrations stabilization. However, we found increases of liver $C_{16:0}$-hexosylceramide in male and female WT mice on FD diet, while CerS6 KO mice showed significantly lower concentrations of this hexosylceramide, indicating that the increase in response to FD diet is coming from the CerS6-generated ceramide. Hexosylceramides are produced via glycosylation of corresponding ceramides, thus the increase of $C_{16:0}$-hexosylceramide apparently masked the increase in production of ceramide by CerS6.

$C_{14:0}$-hexosylceramide was significantly higher in females than in males for both genotypes fed FD diet, while $C_{16:0}$-hexosylceramide was also higher in females than in males for WT mice regardless of diet, and showed no significant difference in KO mice, pointing to sex-specific regulation of liver $C_{16:0}$-ceramide by CerS6 (Figure 4). Interestingly, hexosylceramides were overall less sensitive to folate depletion in males than females. Total HexCer showed a stepwise decrease with increasing dietary FA for male WT and KO mice and female WT mice. Female KO mice, however, had significantly elevated total HexCer on FD diet while levels in mice fed Ctrl or FS diets were very similar (Supplementary Figure 8). The consequences of this response are not clear at present. Hexosylceramides are the simplest members and precursors for a whole class of membrane lipids, the glycosphingolipids [64]. Only glucose or galactose can be added to ceramide head group in mammalian cells [65] and 85% of complex sphingolipids have glucose as a first sugar [66]. Apart from serving as basic substrates for building complex glycosphingolipids, hexosylceramides also have their own biochemical functions. Glucosylceramide is required for intracellular membrane transport, involved in control of cell proliferation and survival, multidrug resistance, natural killer T-cell functions, while galactosylceramide plays major role in myelin formation, promotion of immunotolerance and induction of cytokines [65]. Unfortunately, our analysis did not differentiate between glucosyl- and galactosylceramide.

Our cell-culture studies implied that only CerS6 responded to folate supplementation [14]. The observed increased concentrations of ceramides with longer acyl chains in KO males could be explained by the compensatory mechanisms induced upon the knockout, similar to those observed in cultured cells upon individual CerS knockdown [67]. In cultured cells, CerS6 knockdown was accompanied by upregulation of CerS1, CerS4 and CerS5 producing C_{18}-; C_{18}- C_{20}- and C_{14}- C_{16}- ceramides correspondingly. Such up-regulation could explain medium-long-chain ceramide elevation in our KO mice. At the same time, increase in expression of CerS5 in the knock-out could also favor hetero-dimerization of CerS5 and CerS2 (shown in cultured cells), which had increased activity of CerS5 by a fraction, and activity of CerS2 three-fold in CerS6$^{-/-}$ cells [68]. Thus, heterodimerization mechanism could also account for the increase in very-long-chain ceramides in the KO males. Overall, due to such compensatory changes of ceramide concentrations in males and rather limited ceramide responses in females, total ceramide concentration remained fairly similar among groups although female KO mice fed FD diet had significantly elevated total Cer concentrations compared to KO FS group (Supplementary Figure 7).

Of note, we observed increase of multiple SM species on FS diet which was sex-specific for long chain sphingomyelins but showed no sex differences for very-long-chain sphingomyelins. The increase in SMs on FA over-supplemented diet could be explained by the function of folate metabolism as a supplier of methyl groups for the metabolic processes, including the formation of phosphatidylcholine (PC) from phosphatidylethanolamine (PE) via PEMT pathway [69, 70], with phosphatidylcholine donating the phosphocholine group for the biosynthesis of SM.

Overall, our study has shown that dietary FA affects ceramides as well as complex sphingolipids in both sex and genotype-dependent manner. Sphingolipids, and ceramides in particular, are established regulators of proliferation, differentiation, senescence and apoptosis. Thus, it is reasonable to conclude that alteration of dietary FA could have an effect on these important cellular processes. Sex differences in sphingolipid response observed in our experiments are also in agreement with conclusions from a study of the relationship between hepatic ceramides and insulin resistance in the Hybrid Mouse Diversity Panel [71]. This work has found large differences in genetic, hormonal and dietary regulation of liver $C_{16:0}$-, $C_{18:0}$- and $C_{20:0}$-ceramides indicating that different ceramides have different effects in males and females. It also demonstrated that part of the sex differences could be explained by inhibitory effect of testosterone on the expression of sphingolipid biosynthesis enzymes, such as *Sptlc1, CerS6, Degs1, Asah1, Cerk* and *Kdsr* [71]. Additionally, sex-specific associations of several genomic loci with $C_{16:0}$-, $C_{18:0}$- and $C_{20:0}$-ceramides were found. Sex-specific differences in sphingolipid metabolism in the aging human brains [72] and sex-specific regulation of CerS6 in a study of experimental autoimmune encephalomyelitis [73] have also been reported. It should be noted that evidence for sex-specific regulation and function of sphingolipids has been accumulating since 1985 [74], however the information regarding sex-dependent activity and regulation of sphingolipids (as well as their mechanisms) is still scarce. Thus, investigation of sphingolipid effects, as well as approaches to target them, need to be evaluated mechanistically in each sex.

We employed untargeted metabolomics to investigate how broadly the response to dietary FA affects liver metabolism. Anova comparisons of the main effects of genotype, gender and diet revealed that sex was the strongest factor separating the liver metabolomes (356 from 736 measured metabolites were different between sexes with a $p<0.0001$), while genotype and diet were weaker discriminators (106 metabolites showed differences between genotypes and 67 were different between diets, all with the $p<0.001$). Moreover, three-way ANOVA analysis demonstrated that the three factors differentiating our mouse groups, genotype, sex and diet interact with each other. Thus, 19% of metabolites showed genotype:sex interaction, 14.7% showed sex:diet interaction and 11.7 % metabolites exhibited genotype:diet interaction (Supplementary Tables 10–12), with at least 6% of total measured metabolites manifesting interaction of all three factors (Supplementary Table 13). Among the top 30 biochemicals important for separating liver metabotypes of the groups are the C_{16}-acyl chain containing ceramides, SMs and glucosyl-ceramides, folate coenzymes, FIGLU and gamma-glutamyl-peptides. All of them are directly linked to the effect of genotype and dietary FA (Supplementary Tables 8 & 9). Additionally, changes in phosphoethanolamines (Table 1), as well as diacylglycerols and long chain fatty acids (Supplementary Tables 4 & 5) indicate broader effects on liver metabotype. Apparently, changes in sphingolipid biosynthesis due to the absence of CerS6 altered free fatty acid utilization as well as phospholipid homeostasis.

We acknowledge that our current study has limitations such as measurement of sphingolipid pools in liver but not in plasma or other tissues, as well as the lack of differentiation between glucosyl and galactosyl ceramides. Nevertheless, it successfully tested our hypothesis and presented a significant amount of biochemical data, some of which are unexpected and warrant further investigation, but nevertheless are very important for understanding of how essential nutrient for folate pathway can communicate with multiple other pathways in the whole organism.

5. Conclusion

In conclusion, our study experimentally confirmed the hypothesis that dietary folic acid depletion or over-supplementation affect ceramides and complex sphingolipids in mouse liver and that CerS6 plays a central role in this adaptation. Sphingolipid response to dietary folic acid in our study depended on sex and CerS6 genotype. Moreover, sphingolipids with C_{14}- and C_{16}-acyl chains were found at significantly higher concentrations in female than in male livers. This finding underscores the need for establishing sex-specific reference values for sphingolipid biomarkers and for identifying sex-specific mechanisms of their regulation.

Additionally, while CerS6 and CerS5 are being increasingly implicated in development of obesity and metabolic syndrome [54, 55, 57], the data regarding both short- and long-term effects of dietary micronutrient changes on sphingolipid levels are limited. Precise understanding of how sphingolipids respond to diet is imperative for translating the studies targeting sphingolipids into therapies for humans. Despite the fact that folate is required in relatively small quantities in the diet, it is clearly affecting both sphingolipid and overall liver metabolism.

Our untargeted metabolomic analysis indicates that both dietary folic acid and CerS6 knockout have pleiotropic effects on liver metabolome. Further studies of the mechanisms connecting folate and sphingolipid metabolism as well as characterization of the effects of dietary FA on liver metabolic pathways may help to avoid potential unwanted side-effects of over-supplementation.

Supplementary Material

Refer to Web version on PubMed Central for supplementary material.

ACKNOWLEDGEMENTS

The authors thank Dr. D. Horita for fruitful discussions and for reading and editing the manuscript. The work presented in this manuscript was supported by the National Institutes of Health grant CA193782 to N.K., and B.O. was supported by CA203628, CA214461 and DE016572. Lipidomics Shared Resource Facility was supported by the National Institute of Health Grants P20 RR017677 (SC Lipidomics and Pathobiology COBRE) and P30 CA138313 (Hollings Cancer Center) and C06 RR018823 (National Center for Research Resources and Office of Director of the NIH).

Abbreviations

CerS	Ceramide Synthase
SM	Sphingomyelin
S1P	Sphingosine-1-phosphate
WT	Wild type
KO	Knock-out
FD	Folate deficient
Ctrl	Control
FS	Folate over-supplemented
FA	Folic Acid
7,8-DHF	7,8-dihydrofolate
THF	Tetrahydrofolate
FIGLU	Formiminoglutamate
MTHFR	Methylenetetrahydrofolate reductase

REFERENCES

1. Wagner C, Biochemical role of folate in cellular metabolism, in Folate in Health and Disease, Bailey LB, Editor. 1995, Marcel Dekker, Inc.: New York. p. 23–42.
2. Strickland KC, Krupenko NI, and Krupenko SA, Molecular mechanisms underlying the potentially adverse effects of folate. Clin Chem Lab Med, 2013. 51(3): p. 607–16. [PubMed: 23241610]
3. Scaglione F and Panzavolta G, Folate, folic acid and 5-methyltetrahydrofolate are not the same thing. Xenobiotica, 2014. 44(5): p. 480–8. [PubMed: 24494987]

4. da Silva RP, et al. , Novel insights on interactions between folate and lipid metabolism. Biofactors, 2014. 40(3): p. 277–83. [PubMed: 24353111]
5. Medici V and Halsted CH, Folate, alcohol, and liver disease. Mol Nutr Food Res, 2013. 57(4): p. 596–606. [PubMed: 23136133]
6. Lucock M, Folic acid: nutritional biochemistry, molecular biology, and role in disease processes. Mol Genet Metab, 2000. 71(1-2): p. 121–38. [PubMed: 11001804]
7. McNulty H, et al. , Addressing optimal folate and related B-vitamin status through the lifecycle: health impacts and challenges. Proc Nutr Soc, 2019. 78(3): p. 449–462. [PubMed: 31155015]
8. Au KS, Findley TO, and Northrup H, Finding the genetic mechanisms of folate deficiency and neural tube defects-Leaving no stone unturned. Am J Med Genet A, 2017. 173(11): p. 3042–3057. [PubMed: 28944587]
9. Sid V, Siow YL, and O K, Role of folate in nonalcoholic fatty liver disease. Can J Physiol Pharmacol, 2017. 95(10): p. 1141–1148. [PubMed: 28460180]
10. Lucock M and Yates Z, Folic acid fortification: a double-edged sword. Curr Opin Clin Nutr Metab Care, 2009. 12(6): p. 555–64. [PubMed: 19726978]
11. Christensen KE, et al. , High folic acid consumption leads to pseudo-MTHFR deficiency, altered lipid metabolism, and liver injury in mice. Am J Clin Nutr, 2015. 101(3): p. 646–58. [PubMed: 25733650]
12. Naderi N and House JD, Recent Developments in Folate Nutrition. Adv Food Nutr Res, 2018. 83: p. 195–213. [PubMed: 29477222]
13. Maruvada P, et al. , Knowledge gaps in understanding the metabolic and clinical effects of excess folates/folic acid: a summary, and perspectives, from an NIH workshop. Am J Clin Nutr, 2020. 112(5): p. 1390–1403. [PubMed: 33022704]
14. Hoeferlin LA, et al. , Folate stress induces apoptosis via p53-dependent de novo ceramide synthesis and up-regulation of ceramide synthase 6. J Biol Chem, 2013. 288(18): p. 12880–90. [PubMed: 23519469]
15. Fekry B, et al. , Ceramide Synthase 6 Is a Novel Target of Methotrexate Mediating Its Antiproliferative Effect in a p53-Dependent Manner. PLoS One, 2016. 11(1): p. e0146618. [PubMed: 26783755]
16. Hannun YA and Obeid LM, Sphingolipids and their metabolism in physiology and disease. Nat Rev Mol Cell Biol, 2017.
17. Castro BM, Prieto M, and Silva LC, Ceramide: a simple sphingolipid with unique biophysical properties. Prog Lipid Res, 2014. 54: p. 53–67. [PubMed: 24513486]
18. Goni FM, Sot J, and Alonso A, Biophysical properties of sphingosine, ceramides and other simple sphingolipids. Biochem Soc Trans, 2014. 42(5): p. 1401–8. [PubMed: 25233422]
19. Stith JL, Velazquez FN, and Obeid LM, Advances in determining signaling mechanisms of ceramide and role in disease. J Lipid Res, 2019. 60(5): p. 913–918. [PubMed: 30846529]
20. Senkal CE, et al. , Alteration of ceramide synthase 6/C16-ceramide induces activating transcription factor 6-mediated endoplasmic reticulum (ER) stress and apoptosis via perturbation of cellular Ca2+ and ER/Golgi membrane network. J Biol Chem, 2011. 286(49): p. 42446–58. [PubMed: 22013072]
21. Hannun YA and Obeid LM, Principles of bioactive lipid signalling: lessons from sphingolipids. Nat Rev Mol Cell Biol, 2008. 9(2): p. 139–50. [PubMed: 18216770]
22. Ogretmen B, Sphingolipid metabolism in cancer signalling and therapy. Nat Rev Cancer, 2018. 18(1): p. 33–50. [PubMed: 29147025]
23. Chaurasia B, et al. , Targeting a ceramide double bond improves insulin resistance and hepatic steatosis. Science, 2019. 365(6451): p. 386–392. [PubMed: 31273070]
24. Mullen TD, Hannun YA, and Obeid LM, Ceramide synthases at the centre of sphingolipid metabolism and biology. Biochem J, 2012. 441(3): p. 789–802. [PubMed: 22248339]
25. Haughey NJ, et al. , Roles for dysfunctional sphingolipid metabolism in Alzheimer's disease neuropathogenesis. Biochim Biophys Acta, 2010. 1801(8): p. 878–86. [PubMed: 20452460]
26. Poss AM, Holland WL, and Summers SA, Risky lipids: refining the ceramide score that measures cardiovascular health. Eur Heart J, 2019.

27. Snider JM, Luberto C, and Hannun YA, Approaches for probing and evaluating mammalian sphingolipid metabolism. Anal Biochem, 2019. 575: p. 70–86. [PubMed: 30917945]
28. Levy M and Futerman AH, Mammalian ceramide synthases. IUBMB Life, 2010. 62(5): p. 347–56. [PubMed: 20222015]
29. Zelnik ID, et al. , A Stroll Down the CerS Lane. Adv Exp Med Biol, 2019. 1159: p. 49–63. [PubMed: 31502199]
30. Brachtendorf S, El-Hindi K, and Grosch S, Ceramide synthases in cancer therapy and chemoresistance. Prog Lipid Res, 2019. 74: p. 160–185. [PubMed: 30953657]
31. Hannun YA and Obeid LM, Many ceramides. J Biol Chem, 2011. 286(32): p. 27855–62. [PubMed: 21693702]
32. Nikolova-Karakashian M, Alcoholic and non-alcoholic fatty liver disease: Focus on ceramide. Adv Biol Regul, 2018. 70: p. 40–50. [PubMed: 30455063]
33. Nikolova-Karakashian M, Sphingolipids at the Crossroads of NAFLD and Senescence. Adv Cancer Res, 2018. 140: p. 155–190. [PubMed: 30060808]
34. Samuel VT and Shulman GI, Nonalcoholic Fatty Liver Disease, Insulin Resistance, and Ceramides. N Engl J Med, 2019. 381(19): p. 1866–1869. [PubMed: 31693811]
35. Yki-Jarvinen H, Ceramides: A Cause of Insulin Resistance in Nonalcoholic Fatty Liver Disease in Both Murine Models and Humans. Hepatology, 2020. 71(4): p. 1499–1501. [PubMed: 31899812]
36. Cingolani F, Futerman AH, and Casas J, Ceramide synthases in biomedical research. Chem Phys Lipids, 2016. 197: p. 25–32. [PubMed: 26248326]
37. Park JW, Park WJ, and Futerman AH, Ceramide synthases as potential targets for therapeutic intervention in human diseases. Biochim Biophys Acta, 2014. 1841(5): p. 671–81. [PubMed: 24021978]
38. Sofi MH, et al. , Ceramide synthesis regulates T cell activity and GVHD development. JCI Insight, 2017. 2(10).
39. Wegner MS, et al. , The enigma of ceramide synthase regulation in mammalian cells. Prog Lipid Res, 2016. 63: p. 93–119. [PubMed: 27180613]
40. Holmes RS, Barron KA, and Krupenko NI, Ceramide Synthase 6: Comparative Analysis, Phylogeny and Evolution. Biomolecules, 2018. 8(4).
41. Hernandez-Corbacho MJ, et al. , Tumor Necrosis Factor-alpha (TNFalpha)-induced Ceramide Generation via Ceramide Synthases Regulates Loss of Focal Adhesion Kinase (FAK) and Programmed Cell Death. J Biol Chem, 2015. 290(42): p. 25356–73. [PubMed: 26318452]
42. Oleinik NV, et al. , Rho GTPases RhoA and Rac1 Mediate Effects of Dietary Folate on Metastatic Potential of A549 Cancer Cells through the Control of Cofilin Phosphorylation. J Biol Chem, 2014.
43. Bielawski J, et al. , Comprehensive quantitative analysis of bioactive sphingolipids by high-performance liquid chromatography-tandem mass spectrometry. Methods Mol Biol, 2009. 579: p. 443–67. [PubMed: 19763489]
44. Evans AM, Bridgewater BR, Liu Q, Mitchell MW, Robinson RJ, Dai H, Stewart SJ, DeHaven CD and Miller LAD, High Resolution Mass Spectrometry Improves Data Quantity and Quality as Compared to Unit Mass Resolution Mass Spectrometry in High-Throughput Profiling Metabolomics. Metabolomics, 2014. 4(2): p. 1–7.
45. Ford L, et al. , Precision of a Clinical Metabolomics Profiling Platform for Use in the Identification of Inborn Errors of Metabolism. J Appl Lab Med, 2020. 5(2): p. 342–356. [PubMed: 32445384]
46. Luhby AL, Cooperman JM, and Teller DN, Urinary excretion of formiminoglutamic acid: application in diagnosis of clinical folic acid deficiency. Am J Clin Nutr, 1959. 7: p. 397–406. [PubMed: 14418803]
47. Suh JR, Herbig AK, and Stover PJ, New perspectives on folate catabolism. Annu Rev Nutr, 2001. 21: p. 255–82. [PubMed: 11375437]
48. Hou Z and Matherly LH, Biology of the major facilitative folate transporters SLC19A1 and SLC46A1. Curr Top Membr, 2014. 73: p. 175–204. [PubMed: 24745983]
49. Matherly LH, Hou Z, and Deng Y, Human reduced folate carrier: translation of basic biology to cancer etiology and therapy. Cancer Metastasis Rev, 2007. 26(1): p. 111–28. [PubMed: 17334909]

50. Obeid R, Holzgreve W, and Pietrzik K, Is 5-methyltetrahydrofolate an alternative to folic acid for the prevention of neural tube defects? J Perinat Med, 2013. 41(5): p. 469–83. [PubMed: 23482308]
51. Farrell CJ, Kirsch SH, and Herrmann M, Red cell or serum folate: what to do in clinical practice? Clin Chem Lab Med, 2013. 51(3): p. 555–69. [PubMed: 23449524]
52. Hartman BA, et al. , Neither folic acid supplementation nor pregnancy affects the distribution of folate forms in the red blood cells of women. J Nutr, 2014. 144(9): p. 1364–9. [PubMed: 24991041]
53. Williams B, et al. , A novel role for ceramide synthase 6 in mouse and human alcoholic steatosis. FASEB J, 2018. 32(1): p. 130–142. [PubMed: 28864659]
54. Turpin SM, et al. , Obesity-induced CerS6-dependent C16:0 ceramide production promotes weight gain and glucose intolerance. Cell Metab, 2014. 20(4): p. 678–86. [PubMed: 25295788]
55. Raichur S, et al. , The role of C16:0 ceramide in the development of obesity and type 2 diabetes: CerS6 inhibition as a novel therapeutic approach. Mol Metab, 2019. 21: p. 36–50. [PubMed: 30655217]
56. Turpin-Nolan SM, et al. , CerS1-Derived C18:0 Ceramide in Skeletal Muscle Promotes Obesity-Induced Insulin Resistance. Cell Rep, 2019. 26(1): p. 1–10 e7. [PubMed: 30605666]
57. Gosejacob D, et al. , Ceramide Synthase 5 Is Essential to Maintain C16:0-Ceramide Pools and Contributes to the Development of Diet-induced Obesity. J Biol Chem, 2016. 291(13): p. 6989–7003. [PubMed: 26853464]
58. Hammerschmidt P, et al. , CerS6-Derived Sphingolipids Interact with Mff and Promote Mitochondrial Fragmentation in Obesity. Cell, 2019. 177(6): p. 1536–1552 e23. [PubMed: 31150623]
59. Musso G, et al. , Bioactive Lipid Species and Metabolic Pathways in Progression and Resolution of Nonalcoholic Steatohepatitis. Gastroenterology, 2018. 155(2): p. 282–302 e8. [PubMed: 29906416]
60. Siow DL and Wattenberg BW, Mammalian ORMDL proteins mediate the feedback response in ceramide biosynthesis. J Biol Chem, 2012. 287(48): p. 40198–204. [PubMed: 23066021]
61. Vacaru AM, et al. , Sphingomyelin synthase-related protein SMSr controls ceramide homeostasis in the ER. J Cell Biol, 2009. 185(6): p. 1013–27. [PubMed: 19506037]
62. Bourteele S, et al. , Tumor necrosis factor induces ceramide oscillations and negatively controls sphingolipid synthases by caspases in apoptotic Kym-1 cells. J Biol Chem, 1998. 273(47): p. 31245–51. [PubMed: 9813032]
63. Deevska GM, et al. , Novel Interconnections in Lipid Metabolism Revealed by Overexpression of Sphingomyelin Synthase-1. J Biol Chem, 2017. 292(12): p. 5110–5122. [PubMed: 28087695]
64. van Meer G, Wolthoorn J, and Degroote S, The fate and function of glycosphingolipid glucosylceramide. Philos Trans R Soc Lond B Biol Sci, 2003. 358(1433): p. 869–73. [PubMed: 12803919]
65. Merrill AH Jr., Sphingolipid and glycosphingolipid metabolic pathways in the era of sphingolipidomics. Chem Rev, 2011. 111(10): p. 6387–422. [PubMed: 21942574]
66. Shayman JA, Targeting Glucosylceramide Synthesis in the Treatment of Rare and Common Renal Disease. Semin Nephrol, 2018. 38(2): p. 183–192. [PubMed: 29602400]
67. Mullen TD, et al. , Selective knockdown of ceramide synthases reveals complex interregulation of sphingolipid metabolism. J Lipid Res, 2011. 52(1): p. 68–77. [PubMed: 20940143]
68. Laviad EL, et al. , Modulation of ceramide synthase activity via dimerization. J Biol Chem, 2012.
69. Ganz AB, et al. , Genetic impairments in folate enzymes increase dependence on dietary choline for phosphatidylcholine production at the expense of betaine synthesis. FASEB J, 2016. 30(10): p. 3321–3333. [PubMed: 27342765]
70. Reo NV, Adinehzadeh M, and Foy BD, Kinetic analyses of liver phosphatidylcholine and phosphatidylethanolamine biosynthesis using (13)C NMR spectroscopy. Biochim Biophys Acta, 2002. 1580(2-3): p. 171–88. [PubMed: 11880242]
71. Norheim F, et al. , Genetic, dietary, and sex-specific regulation of hepatic ceramides and the relationship between hepatic ceramides and IR. J Lipid Res, 2018. 59(7): p. 1164–1174. [PubMed: 29739864]

72. Couttas TA, et al. , Age-Dependent Changes to Sphingolipid Balance in the Human Hippocampus are Gender-Specific and May Sensitize to Neurodegeneration. J Alzheimers Dis, 2018. 63(2): p. 503–514. [PubMed: 29660940]

73. Eberle M, et al. , Regulation of ceramide synthase 6 in a spontaneous experimental autoimmune encephalomyelitis model is sex dependent. Biochem Pharmacol, 2014. 92(2): p. 326–35. [PubMed: 25173988]

74. Bouchon B, Portoukalian J, and Bornet H, Sex-specific difference of the galabiosylceramide level in the glycosphingolipids of human thyroid. Biochim Biophys Acta, 1985. 836(1): p. 143–52. [PubMed: 4027258]

Highlights

- Over-supplementation with FA depletes liver 5-methyl-tetrahydrofolate.
- Dietary FA affects multiple liver sphingolipid classes in a CerS6-dependent manner.
- Individual sphingolipid species concentrations significantly differ between sexes.
- Folic acid over-supplementation significantly increased multiple sphingomyelins.

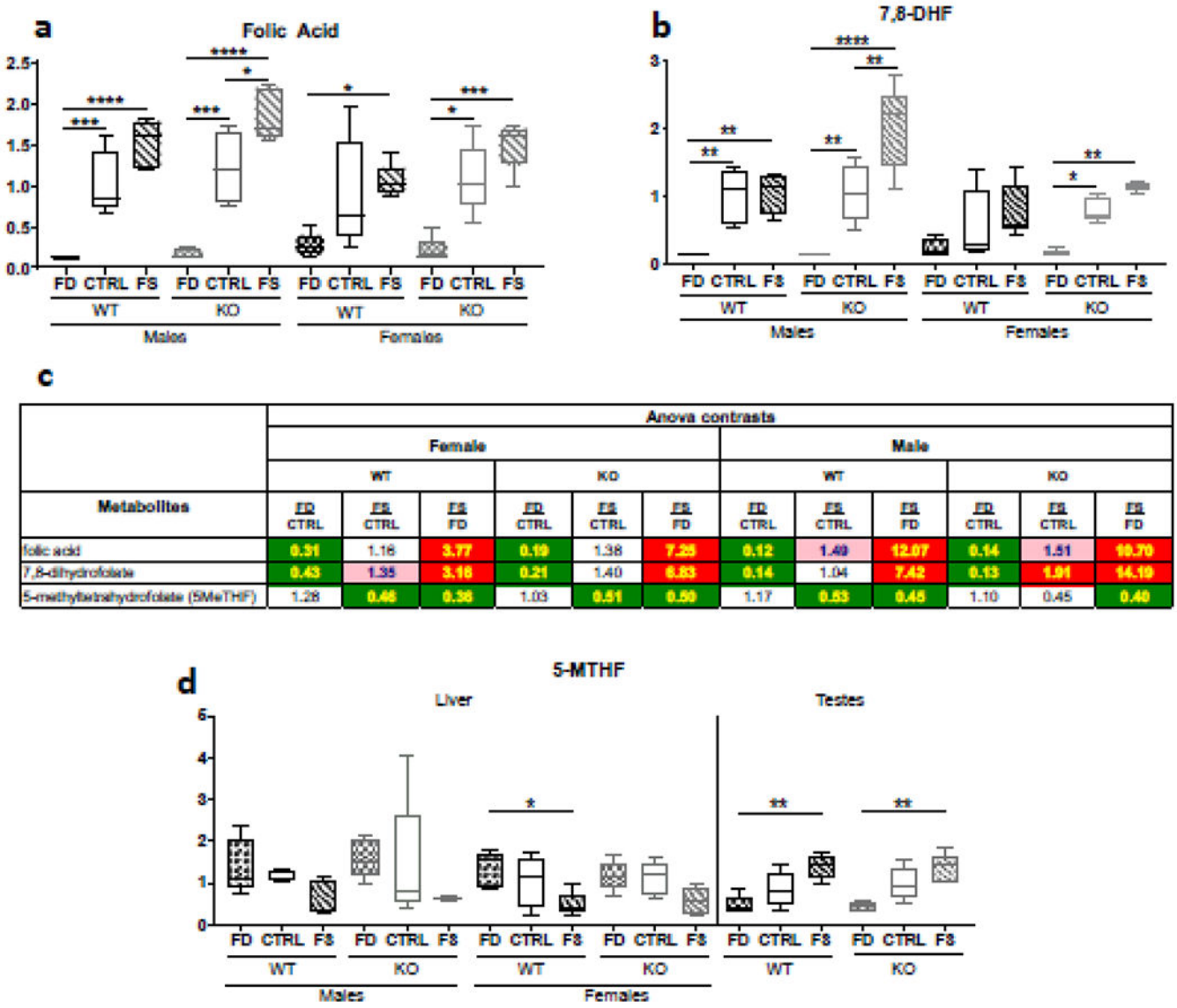

Figure 1.

Alteration of dietary folic acid supplementation differentially affects the concentrations of liver folate derivatives. Tissue folic acid (a), 7,8-dihydrofolic acid (b) and 5-methyl-THF (c) demonstrate distinct dose responses. Fold changes of each metabolite for different comparison groups can be seen in panel (d). Metabolon® measurements presented as box plots showing minimum and maximum values were plotted using Prism software, n=5. Checkered bars, FD diet; solid bars, Control diet; striped bars, FS diet. WT shown in black and KO shown in grey. *, $p<0.05$; **, $p<0.01$; ***, $p<0.001$; ****, $p<0.0001$, determined by One-way ANOVA with Sidak's multiple comparisons test.

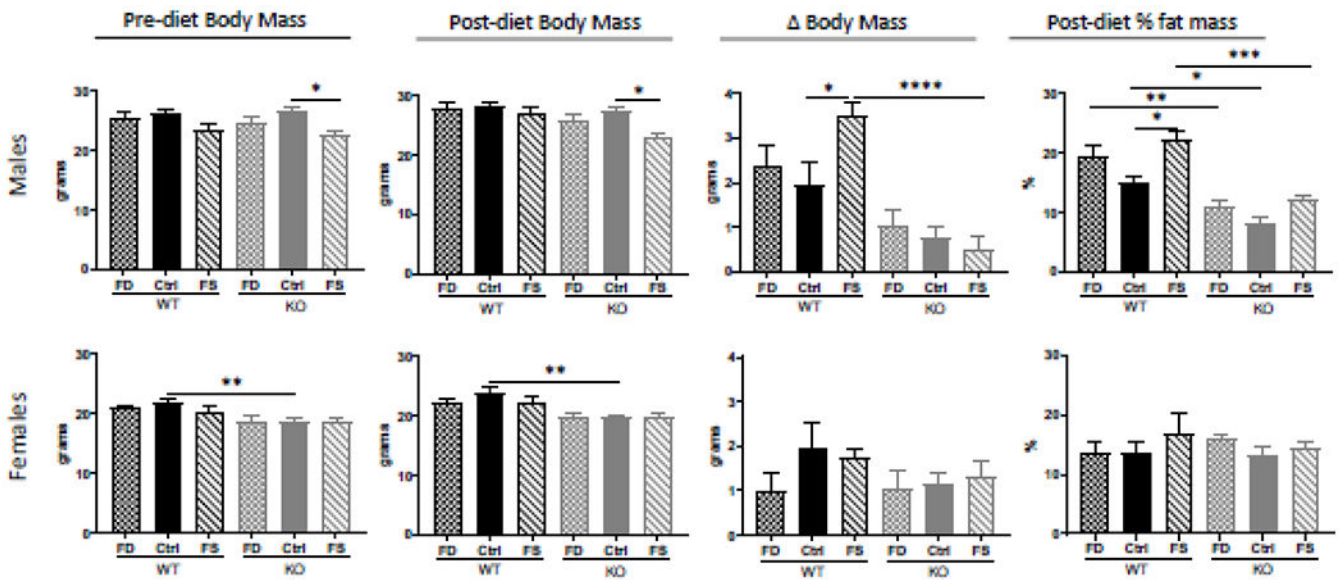

Figure 2.

CerS6 KO male but not female mice gained significantly less weight and fat mass, regardless of dietary folate supplementation. Body mass and composition were measured before and after dietary intervention. Change in body mass was calculated by subtracting pre-diet animal body mass from the post-diet mass. Fat mass was measured by Body Composition Analyzer. Data represent mean ± SEM, n=5. Checkered bars - FD diet; solid bars - Control diet; striped bars - FS diet. WT shown in black and KO shown in grey. *, $p<0.05$; **, $p<0.01$; ***, $p<0.001$; ****, $p<0.0001$, determined by One-way ANOVA with Sidak's multiple comparisons test.

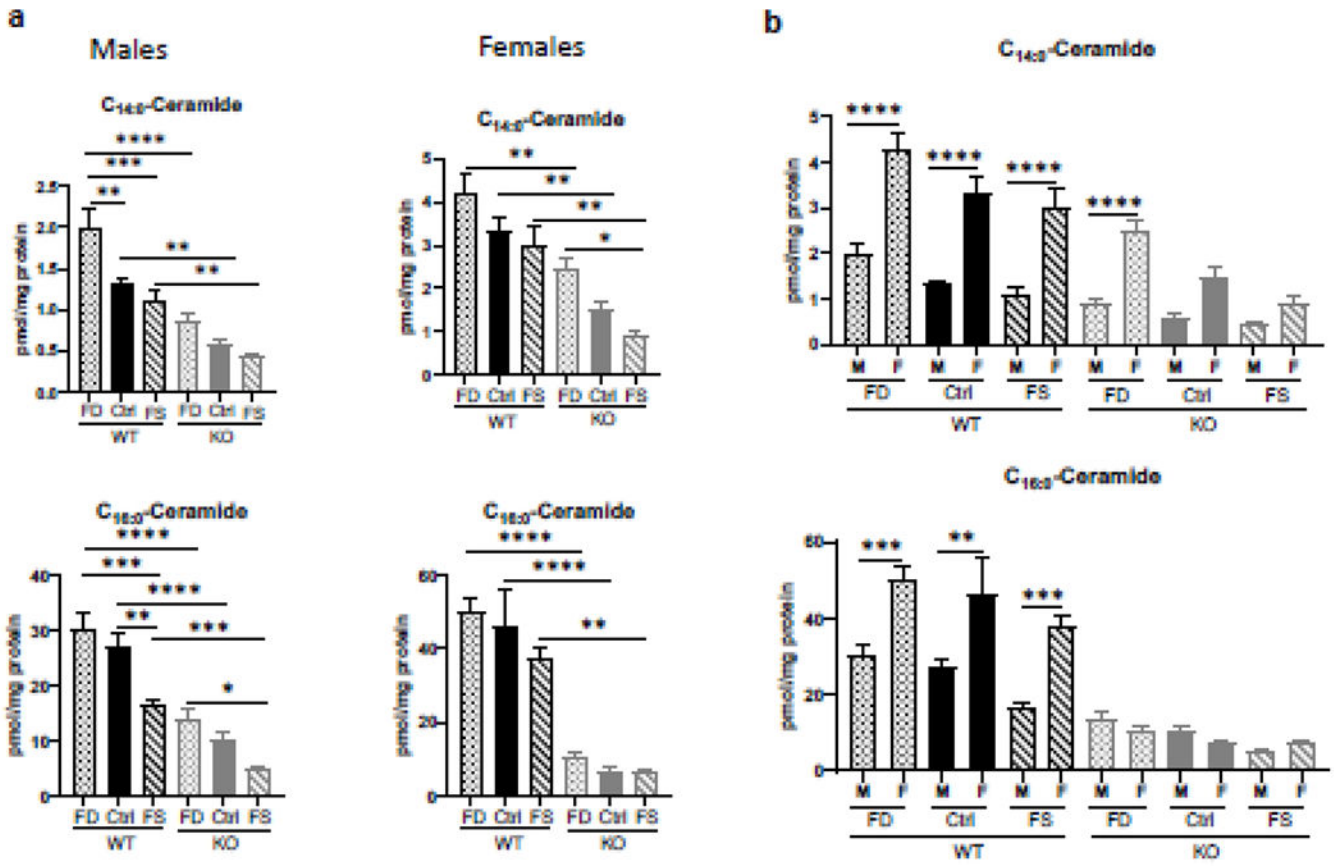

Figure 3.

Sex-specific differences in $C_{14:0}$- and $C_{16:0}$- liver ceramide concentrations and their response to dietary FA. Effect of FA supplementation on $C_{14:0}$- and $C_{16:0}$- ceramide concentrations in WT and CerS6 KO mice (a) and comparison of these ceramide species in male and female mice (b). Data are shown as mean ± SEM, n=5. Checkered bars, FD diet; solid bars, Control diet; striped bars, FS diet. WT shown in black and KO shown in grey. *, $p<0.05$; **, $p<0.01$; ***, $p<0.001$; ****, $p<0.0001$, determined by One-way ANOVA with Sidak's multiple comparisons test.

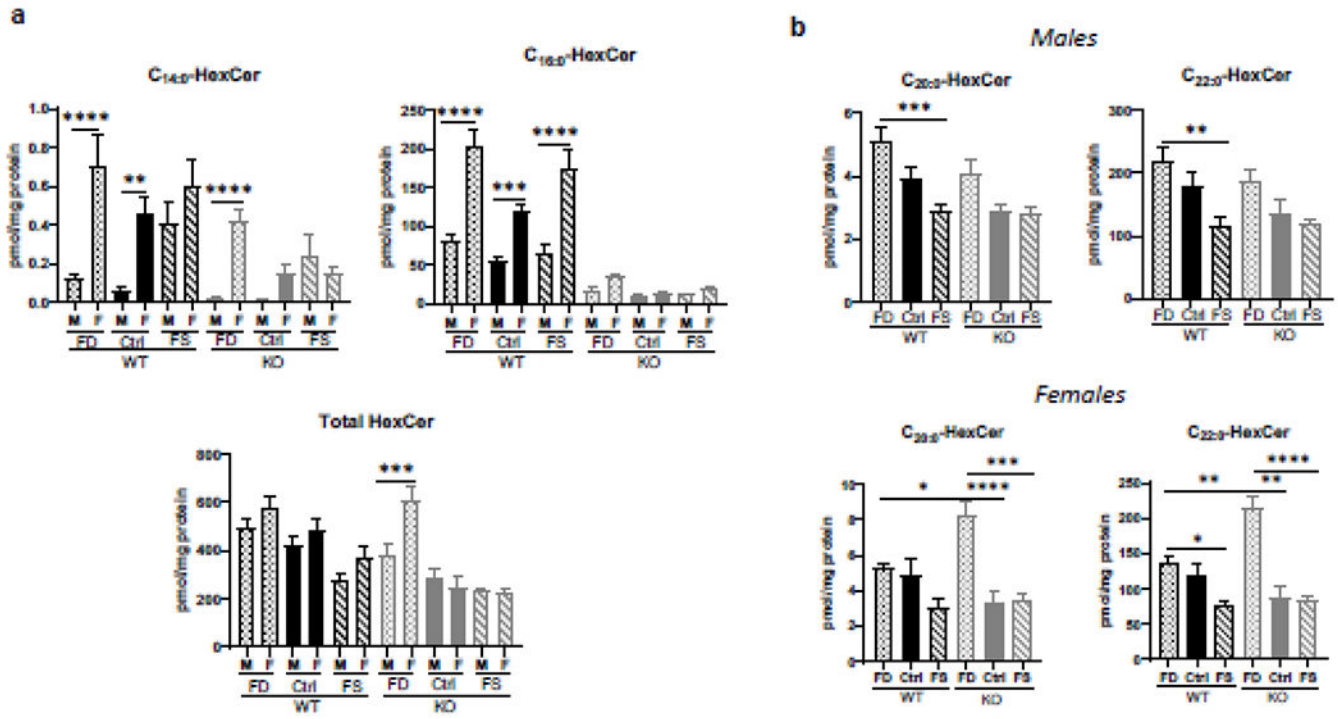

Figure 4.

Sex-specific differences in $C_{14:0}$-, $C_{16:0}$- and $C_{22:0}$- liver hexosylceramide concentrations and their response to dietary FA. Effects of FA supplementation on $C_{14:0}$-, $C_{16:0}$- and total hexosylceramides in males and females (a) and on $C_{20:0}$- and $C_{22:0}$-species (B). Data are shown as mean ± SEM, n=5. Checkered bars, FD diet; solid bars, Control diet; striped bars, FS diet. WT shown in black and KO shown in grey. *, p<0.05; **, p<0.01; ***, p<0.001; ****. p<0.0001, determined by One-way ANOVA with Sidak's multiple comparisons test.

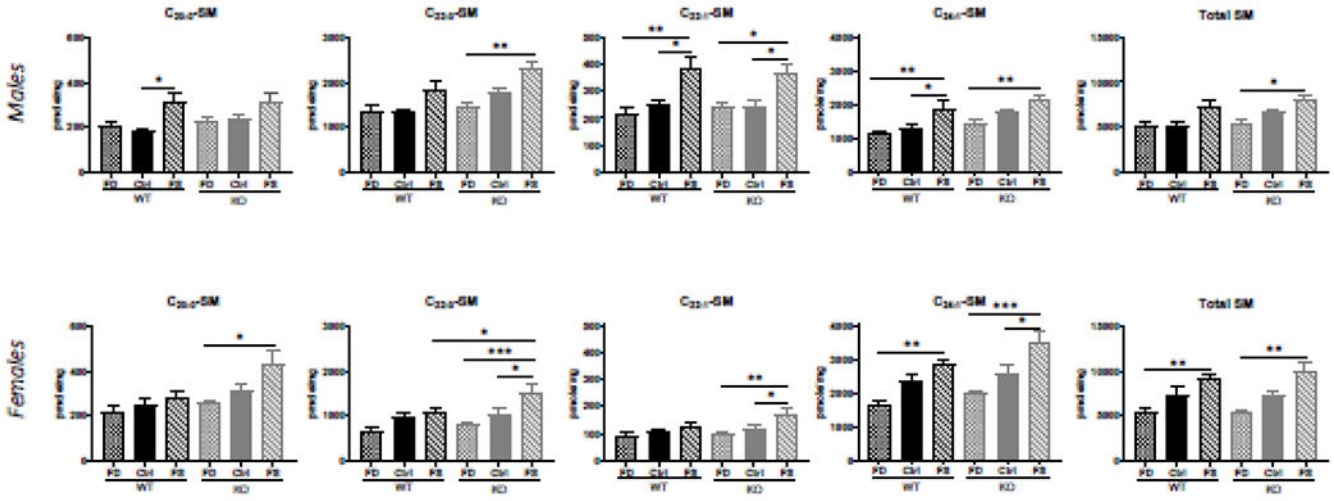

Figure 5.

FA over-supplementation increased very-long-chain sphingomyelin concentrations in WT and CerS6 KO mice of both sexes. Data presented as mean ± SEM, n=5. Checkered bars, FD diet; solid bars, Control diet; striped bars, FS diet. WT shown in black and KO shown in grey. *, $p<0.05$; **, $p<0.01$; ***, $p<0.001$; ****. $p<0.0001$, determined by One-way ANOVA with Sidak's multiple comparisons test.

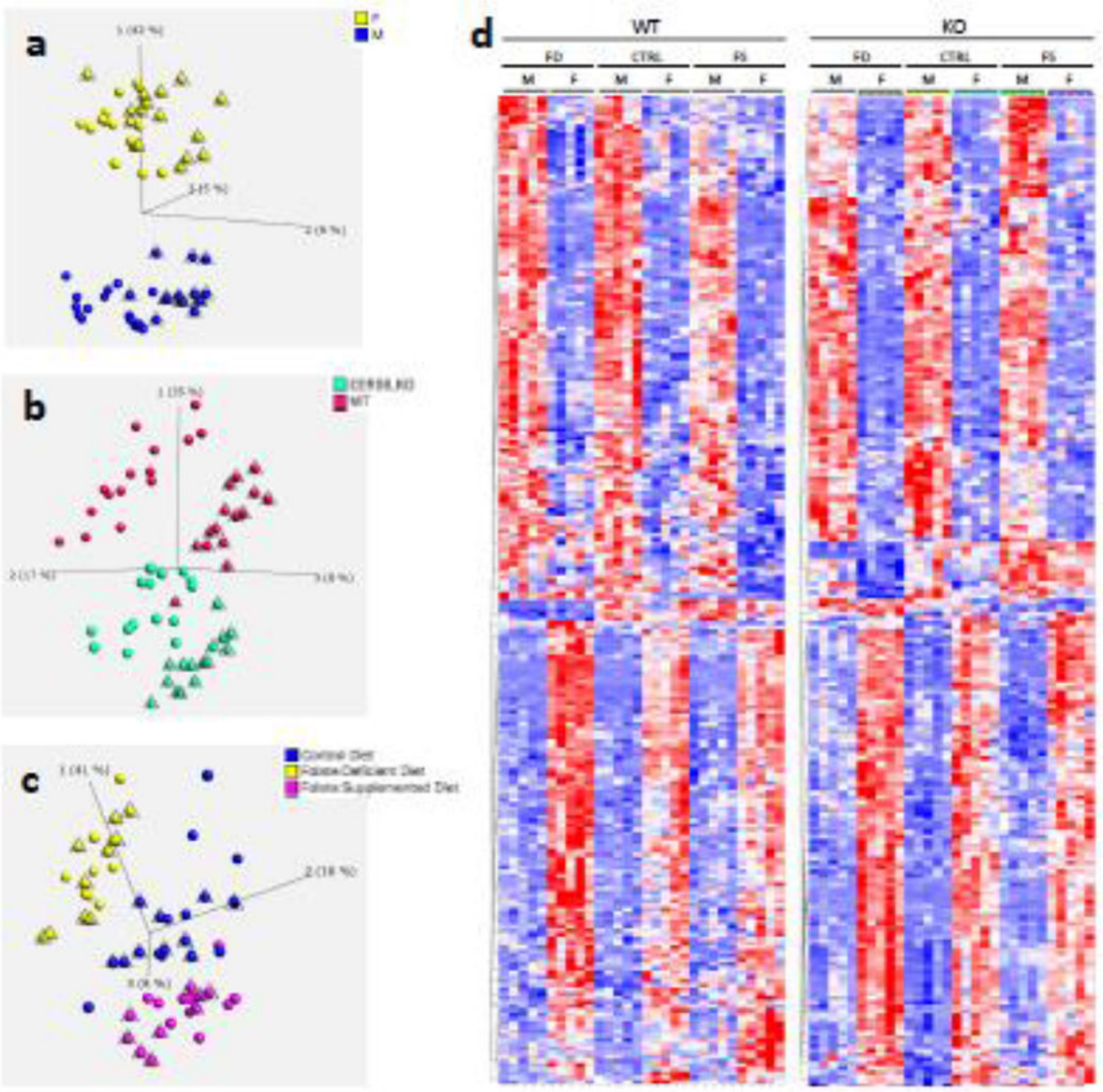

Figure 6.

Clear separation of liver samples by sex (a), genotype (b) and diet (c) by Principal Component Analysis (PCA) of measured metabolites demonstrates. Triangulated spheres represent: WT mice (a), male mice (b), and WT mice (c). Heat Map (HM) analysis (d) demonstrates differences of group's metabotypes. For panel **d**, only metabolite differences with p-value <0.02 were included. Analysis was performed using Qlucore Omics Explorer v.3.4 software.

Table 1.

Multiple liver phosphatidylethanolamine concentrations differ in male vs female livers and are increased by CerS6 KO. Red, p<0.05; pink, p<0.1; green, p<0.05; light geen, p<0.1.

		Anova contrasts											
		Female			Male			Female / Male					
		KO / WT			KO / WT			WT			KO		
Sub Pathway	Metabolites	FD	CTRL	FS	FD	CTRL	FS	FD	CTRL	FS	FD	CTRL	FS
Phosphatidylethanolamine (PE)	1,2-dipalmitoyl-GPE (16:0/16:0)*	1.37	1.17	1.54	1.45	1.09	1.12	1.30	1.30	1.25	1.23	1.40	1.72
	1-palmitoyl-2-stearoyl-GPE (16:0/18:0)*	1.58	0.76	1.38	1.99	0.76	0.63	2.86	3.32	2.04	2.27	3.33	4.44
	1-palmitoyl-2-oleoyl-GPE (16:0/18:1)	1.29	1.15	1.56	1.51	1.32	1.22	0.91	0.71	0.78	0.78	0.61	0.99
	1-palmitoyl-2-linoleoyl-GPE (16:0/18:2)	1.19	1.62	1.67	1.53	1.80	1.66	0.66	0.53	0.61	0.52	0.47	0.61
	1-palmitoyl-2-arachidonoyl-GPE (16:0/20:4)*	1.03	1.11	1.17	1.12	1.14	1.12	0.83	0.77	0.81	0.76	0.75	0.85
	1-palmitoyl-2-docosahexaenoyl-GPE (16:0/22:6)*	1.00	1.07	1.05	1.08	1.14	0.96	1.24	1.19	1.07	1.14	1.12	1.18
	1-stearoyl-2-oleoyl-GPE (18:0/18:1)	1.19	1.00	1.32	1.37	1.17	1.08	1.14	0.94	1.02	0.99	0.80	1.24
	1-stearoyl-2-linoleoyl-GPE (18:0/18:2)*	1.04	1.17	1.42	1.32	1.55	1.40	0.97	0.90	0.91	0.76	0.67	0.92
	1-stearoyl-2-arachidonoyl-GPE (18:0/20:4)	0.98	0.98	1.08	1.07	1.09	1.02	1.01	1.02	0.93	0.93	0.92	0.99
	1-stearoyl-2-docosahexaenoyl-GPE (18:0/22:6)*	0.96	1.08	1.04	1.18	1.36	0.98	1.50	1.41	1.08	1.22	1.13	1.16
	1-oleayl-2-linoleoyl-GPE (18:1/18:2)*	1.22	1.30	1.57	1.39	1.38	1.53	0.65	0.52	0.68	0.57	0.49	0.69
	1-oleoyl-2-arachidonoyl-GPE (18:1/20:4)*	1.08	0.99	1.10	1.14	1.01	0.99	1.01	0.85	0.89	0.95	0.83	0.99
	1-oleoyl-2-docosahexaenoyl-GPE (18:1/22:6)*	1.04	0.96	0.98	1.07	1.02	0.87	1.19	1.07	1.04	1.16	1.01	1.18
	1,2-dilinoleoyl-GPE (18:2/18:2)*	0.98	1.29	1.63	1.63	2.25	2.20	0.59	0.58	0.73	0.35	0.33	0.54
	1-linoleoyl-2-arachidonoyl-GPE (18:2/20:4)*	1.02	1.00	1.27	1.27	1.39	1.37	0.74	0.74	0.83	0.60	0.53	0.77